

Research Article

Study on the Stage Failure Mechanism and Stability Control of Surrounding Rock of Repeated Mining Roadway

Xiangye Wu ^{1,2}, Jingya Wang,¹ Wencai Wang,¹ Chen Tian,³ Qingwei Bu,¹ and Lin Wu¹

¹Institute of Mining Engineering, Inner Mongolia University of Science and Technology, Baotou 014010, China

²School of Energy and Mining Engineering, China University of Mining and Technology (Beijing), Beijing 100083, China

³Bulianta Coal Mine, Shenhua Shendong Coal Group Corporation Limited, Ordos 017209, China

Correspondence should be addressed to Xiangye Wu; 175874171@qq.com

Received 30 July 2020; Revised 9 September 2020; Accepted 16 September 2020; Published 30 September 2020

Academic Editor: Jianping Zuo

Copyright © 2020 Xiangye Wu et al. This is an open access article distributed under the Creative Commons Attribution License, which permits unrestricted use, distribution, and reproduction in any medium, provided the original work is properly cited.

China is one of the leading countries in the mining and utilization of coal resources, and the problems of coal-mining technology and safety have been concerned by the world, while the serious deformation and destruction of surrounding rock and the difficulty of support have brought inconvenience to the mining of coal resources due to repeated mining. This paper takes the actual engineering 22205 mining roadway in Buertai mine as the research background, through the combination of numerical simulation and field measurement. In this paper, the stress environment, plastic zone, and surrounding rock deformation in the advancing process of coal-mining face are studied, and the stress evolution law of surrounding rock in repeated mining roadway is obtained. It is clarified that the surrounding rock deformation is the failure mechanism under the combined action of principal stress difference and stress direction deflection. As a result, the surrounding rock of the roadway is asymmetrically deformed and destroyed, and the corresponding surrounding rock control scheme is put forward. The results show that the influence of repeated mining on roadway stress environment can be divided into four stages with the mining process: the stability stage of mining influence, the expansion stage of primary mining, the stable stage after primary mining, and the expansion stage of second mining. At the same time, the shape changes of the plastic zone and the displacement monitoring results of the monitoring are analyzed, and the results are obtained; the stage of stress change is suitable, and combined with the failure characteristics of surrounding rock in each stage, it is put forward that reinforcement measures should be taken in the stable stage after mining; the specific reinforcement scheme is determined according to the expansion form of plastic zone and field measurement. The on-site monitoring shows that there is no roof fall accident during the use of the roadway, which ensures the safety in production.

1. Introduction

Coal is one of the three major energy sources in the world and accounts for one-third of the global energy consumption. China's coal storage is in the forefront of the world, and its energy consumption mainly comes from coal energy [1, 2]. In order to meet the needs of national development, the mining intensity and depth of coal resources are increasing day by day, and the disasters of mine water inrush and seepage occur more frequently; the following coal-mining technology and safety issues have attracted widespread attention [3–7].

In recent years, the mining intensity of coal mines has been increasing, of which the double-roadway layout is

mostly used in ten million ton coal mines, which reduces the number of moving of coal-mining face, improves the output and efficiency of coal-mining face, solves the problem of long-distance single head driving ventilation, and makes the transportation of coal, materials, and pedestrians more convenient, and the transportation, installation, and withdrawal of coal-mining face equipment are also more convenient; speed up and flexibility create many convenient conditions for the production of the coal-mining face. However, the following is the problem of repeated mining caused by the layout of double roadways. Repeated mining refers to the mining mode in which the surrounding rock of the damaged roadway is again deformed and damaged when the next coal-mining face continues to be mined. In general,

the damage degree of repeated mining is greater than that of the primary mining, which directly affects whether the coal resource mining process can be carried out safely and smoothly. Therefore, the failure mechanism of surrounding rock of the repeated mining roadway is worthy of in-depth study.

To date, a great number of theories have been proposed explaining failure mechanism of roadway surrounding rock, mainly including the following: classical circular plastic zone theory, surrounding rock loose circle theory, natural caving arch theory, axial deformation theory, surrounding rock partition cracking theory, and “butterfly-shaped plastic zone” theory of roadway surrounding rock. Past theories have basically shown that the failure of surrounding rock is caused by the formation and development of the plastic zone of surrounding rock. The malignant expansion of plastic zone is the direct cause of large deformation, loose failure, and support failure of surrounding rock, and the formation of plastic zone is directly related to surrounding rock stress. Based on the above classical theory, in recent years, many scholars have studied the surrounding rock failure of multiroadway layout [8–10]. Based on a large number of measured data, Kang et al. [11] analyzed the deformation and stress distribution characteristics of the surrounding rock of the remaining roadway and proposed that the deformation of the surrounding rock of the remaining roadway mainly occurred in the back of the coal-mining face, and the mining impact range was large. Wang et al. [12, 13] studied the side mining stress field of goaf by using the double-roadway layout coal-mining face retained entry and mastered the deformation law of surrounding rock in different periods of the double-roadway layout coal-mining face retained entry. Liu et al. and Yu et al. [14, 15] studied the stress distribution and change rule of the coal pillars in front of the work and between the side roadways, so as to systematically study the failure rule of the mining process and reasonably determine the size of the coal pillars between the roadways. Hou et al. [16] analyzed the whole process of surrounding rock failure evolution, the law of surrounding rock deformation, and the form of surrounding rock failure in double roadway without support. Guo et al. [17] studied the change rule of the general shape of the plastic zone of the surrounding rock of the circular tunnel, providing the theoretical basis for the engineering practice. Jiang et al. [18–21] studied the design of the width of the coal pillars between the side roadways of the goaf under the condition of crushing, compared the stress distribution, failure expansion, and displacement evolution of the roadways under the condition of different width of the coal pillars in the whole service life, and studied the influence of the width of the coal pillars on the ground stability. Wu et al. [22] studied the repeated mining roadway and obtained the time-space evolution regularity of the plastic zone and stress of the surrounding rock of the repeated mining roadway. Zhang et al. [23, 24] studied the stability of the remaining roadway roof after the backfilling of the mined out area and provided the basis for the design of preventing roof damage. Wang et al. [25, 26] studied the surrounding rock of coal roadway under the action of excavation and unloading of rock mass

and revealed the mechanism of asymmetric large fracture and expansion deformation failure of the surrounding rock of deep buried and gently inclined jointed rock roadway.

The above study on the stability of roadway under the condition of double roadway arrangement provides valuable experience, but the process of failure mechanism and characters of roadway surrounding rock in the process of repeated mining needs further study. In this paper, based on the engineering background of the air return roadway of coal-mining face 22205 in Buertai, through studying the stress evolution of the surrounding rock and the expansion and change of the plastic zone in the roadway, to reveal the stage and the plastic zone failure mechanism in the process of roadway failure, so as to provide the basis for the control method of the surrounding rock and the stability control technology of the surrounding rock in the repeated mining roadway, which has certain theoretical significance to ensure the safe and efficient production of the mine and practical value.

2. Engineering Background

Buertai coal mine is the main modern mine of the Shandong Group, with a design production capacity of 20.0 Mt. The No. 2-2 coal seam is the first coal seam in the panel 2, with a coal seam dip angle of 1° – 3° . The coal-mining face 22205 is about 303 m long and 3.5 m high. The coal-mining face 22204 is about 320 m long and 2.5 m high. The two coal-mining faces arranged along the towards, with full mining height at one time and full caving method to treat the goaf. The width of coal pillar between roadways is 20 m. The return airway is 300 m deep and 4865 m long. The shape of roadway section is rectangular, which is 5400 mm wide and 3400 mm high. When coal-mining face 22204 is mined, it is used as the auxiliary transportation roadway of coal-mining face. When coal-mining face 22205 is mined, the reserved roadway serves as the return airway, which is affected by repeated mining. The return airway 22205 arrangement form in Buertai coal mine is shown in Figure 1.

The lithological column diagram of the roadway surrounding rock and support structure is shown in Figure 2.

The roof of return airway 22205 adopts combined support that makes up of left-hand nonlongitudinal screw steel bolt, steel mesh, anchor cable, and steel belt. The type of anchor bolt is $\Phi 22 \times 2000$ mm, the spacing between rows is 1000×1000 mm, six in a row, and the center of the top anchor bolt at both ends of each row is 200 mm from the roadway side. The type of anchor cable is $\Phi 22 \times 8000$ mm, the spacing between rows is 2100×2000 mm, and there are three cables in each row. The coal wall and coal pillar side are arranged in a “four-row rectangle” way, with a row spacing of 800×1000 mm. The coal wall is supported by FRP bolt, wooden pallet, and plastic mesh, and the type of bolt is $\Phi 22 \times 2100$ mm. The coal pillar side is supported by screw steel bolt, wood tray, and lead wire mesh, and the type of bolt is $\Phi 18 \times 2100$ mm.

As shown in Figure 3, on the basis of on-situ engineering geological condition, it can be seen that due to the influence of mining, there are coal wall spalling and roof falling in the

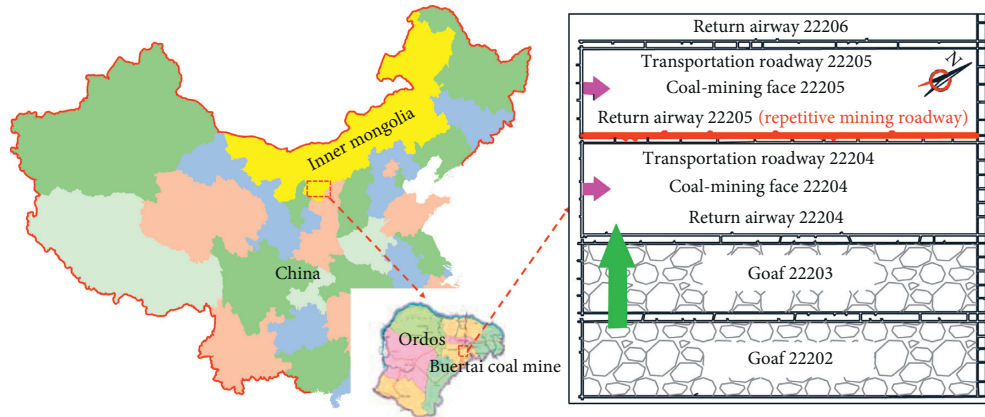


FIGURE 1: Return airway 22205 arrangement form in Buertai coal mine.

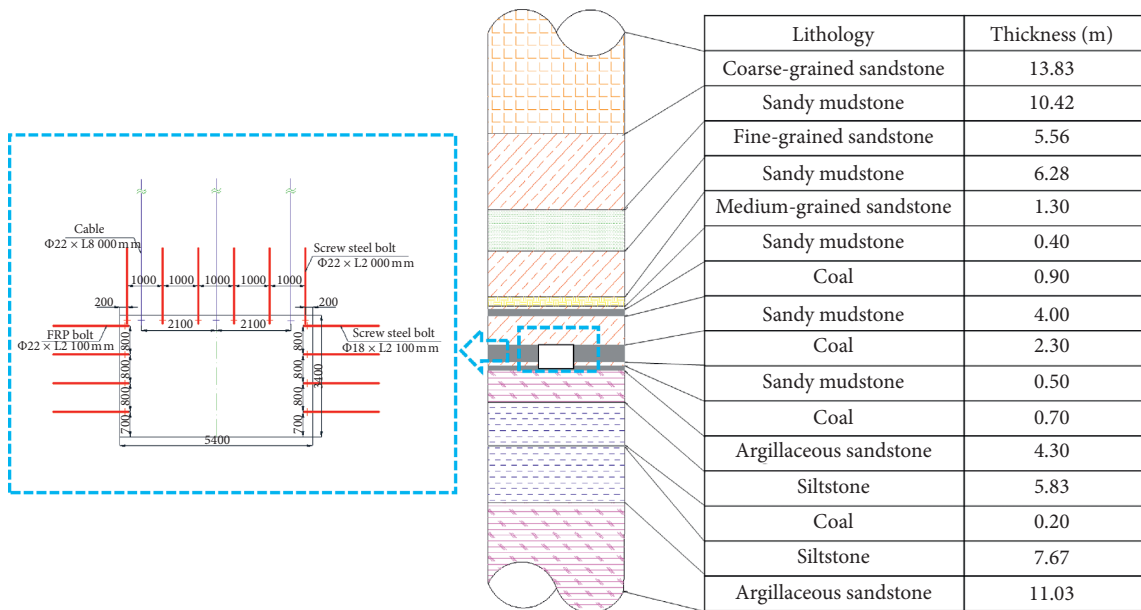


FIGURE 2: Generalized geological column and support structure of roadway.



FIGURE 3: Deformation and failure diagram of surrounding rock on-site. (a) Roof falling. (b) Coal wall spalling.

roadway, and the supporting structure is damaged, which brings potential safety hazards to the site construction.

3. Establishment of Numerical Model

3.1. Double-Yield Model of Goaf. After the longwall face is mined, when the whole caving method is adopted to deal with the goaf, the mining space is filled by the loose rock mass formed by the direct roof caving, forming the caving zone. Under the pressure of the overlying rock, the rock mass in the caving zone is compacted and consolidated, forming the bearing body to be under pressure again. The material in the goaf is characterized by strain hardening, and the bearing capacity of the caving gangue will significantly affect the regularity of stress distribution around the goaf. The double-yield model is applicable to simulate the rock and soil materials that will produce irrecoverable compression deformation and shear yield, and it can be applied to fill the goaf and collapse zone [27].

According to the stress-strain relationship in the compression process of fractured rock mass deduced by Salamon [28, 29], combined with Yavuz [30] based on a large number of rock uniaxial compression test data regression analysis, the initial tangent modulus of rock mass in the collapse zone is obtained, and finally, the stress-strain relationship in the compaction process of rock mass in the collapse zone is obtained:

$$\sigma_V = \frac{10.39\sigma_c^{1.042}}{b^{7.7}} \cdot \frac{\varepsilon_V}{1 - (b/b - 1)\varepsilon_V}. \quad (1)$$

In the equation, σ_V is the vertical stress of the rock block in the goaf, MPa; ε_V is the volume stress variable under the current vertical stress; σ_c is the uniaxial compressive strength, MPa; and b is the coefficient of gangue expansion, which can be obtained from the following equation:

$$b = 1 + \frac{c_1 h + c_2}{100}. \quad (2)$$

Based on the different geological conditions of a large number of mines in China and the United States, Bai et al. obtained statistical regression equation (3) for calculating the height of the caving zone through statistical regression analysis [31]:

$$H = \frac{100h}{c_1 h + c_2}, \quad (3)$$

where H is the mining height, m ; C_1 and C_2 are parameters (Table 1) related to roof lithology [32–34].

According to equation (3) and Table 1, the height of caving zone is related to the mining thickness and direct roof strength of coal seam. Combined with the results of the physical parameters test of coal seam rock in coal-mining face 22205 of Buertai mine, the height of the caving zone in the process of coal seam mining is calculated to be 8.13 m. Then, b is 1.3.

It can be seen from this equation that the stress-strain relationship in the process of rock compaction in the collapse zone is determined by the coefficient of dilatancy b and

TABLE 1: Coefficients for height of caving zone.

Direct roof lithology	Compressive strength (MPa)	C_1	C_2
Hard	>40	2.1	16
Relatively hard	20~40	4.7	19
Soft	<20	6.2	32

σ_C . The stress-strain relationship of materials in goaf calculated by Salamon is shown in Table 2.

In order to obtain the parameters of the double-yield model of goaf, the numerical simulation uniaxial compression test is carried out. The unit block is a cube with a side length of 1 m, with fixed displacement around and at the bottom of the model, and fixed vertical velocity loading is applied at the top of the model. Through the trial-and-error inversion method, the material parameter assignment value is adjusted continuously, so that the stress-strain curve of the block outputted by the numerical calculation model and the stress-strain curve of the theoretical model are obtained. The results are shown in Figure 4.

Through the comparison between the theoretical equation and numerical simulation of the stress-strain relationship of a unit in the goaf as shown in Figure 4, it can be seen that the numerical simulation results are in good agreement with the theoretical equation, and then the double-yield model parameters of the caving zone are obtained, as shown in Table 3.

3.2. Feasibility Analysis of Double-Yield Model in Goaf.

Based on the engineering geological conditions of Buertai coal mine, the numerical model size is 1000 m × 1400 m × 100 m ($x \times y \times z$). Therefore, the vertical initial stress of the coal seam is simulated. According to the burial depth of 300 m, a vertical load of 5.5 MPa is applied to the upper part of the model, and the self-weight of the overlying loose layer is simulated. The surrounding and bottom of the model are fixed constraints. Initial command is adopted for horizontal initial stress, with an initial value of −8 MPa and gradient value of 0.025 MPa. The numerical calculation model is shown in Figure 5.

On the basis of laboratory rock mechanics experiment, certain reduction coefficient is determined according to different weights, so as to obtain rock mechanics parameters that are more consistent with the actual situation on-site. Within the scope of the calculation model, the treatment of rock layers is simplified with similar physical properties and they are combined. Table 4 shows rock mechanics parameters.

A vertical stress monitoring line A-A is arranged along the y -axis direction (trend) in the middle of the coal-mining face to monitor the distribution rule of the vertical stress in the goaf during the mining of the coal-mining face. The vertical stress is extracted every 100 m, and the generated curve is shown in Figure 6.

When the coal-mining face advances 100 m, the vertical stress in the middle of the goaf reaches about 2 MPa and recovers to 26% of the original rock stress. With the continuous mining of the coal-mining face, the vertical

TABLE 2: Relationship between stress and strain for gob material in the double-yield model.

Strain	Stress (MPa)	Strain	Stress (MPa)	Strain	Stress (MPa)
0.01	0.33	0.08	3.83	0.15	13.40
0.02	0.68	0.09	4.61	0.16	16.31
0.03	1.08	0.10	5.52	0.17	20.18
0.04	1.51	0.11	6.57	0.18	25.6
0.05	2.00	0.12	7.81	0.19	33.61
0.06	2.53	0.13	9.31	0.20	46.88
0.07	3.14	0.14	11.12	0.21	72.92

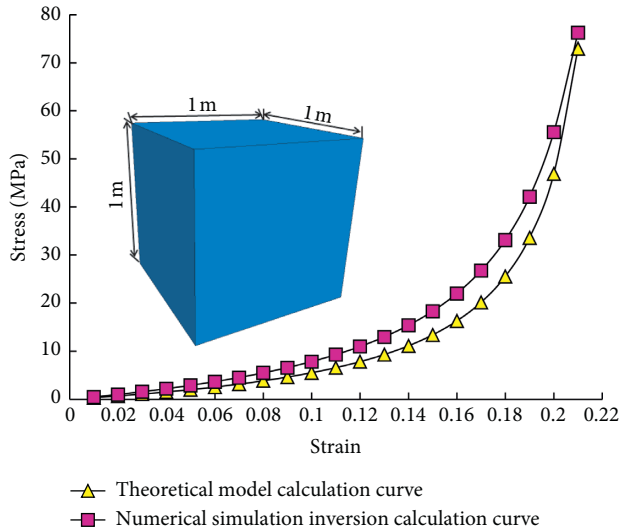


FIGURE 4: Numerical simulation inversion and theoretical calculation of stress-strain relationship in the collapse zone.

stress in the middle of the goaf increases gradually, until the coal-mining face advances to 400 m, and the vertical stress in the middle of the goaf recovers to the original rock stress. The field study shows that [35], when the goaf is restored to the original rock stress state, the distance between the goaf and the coal-mining face is 0.12–0.6 times of the coal seam buried depth, and the numerical simulation results are consistent with the field calculation results, so as to improve the reliability of the numerical simulation of the plastic area and stress field of the surrounding rock of the mining roadway.

4. Distribution Characteristics of Deformation Stages of Surrounding Rock in Repeated Mining Roadway

The influence of repeated mining on roadway is a dynamic evolution process. With the advance of coal-mining face in each position of roadway, the damage degree of surrounding rock changes accordingly, showing a certain stage of change. According to the field mining sequence, the mining process is simulated to study the stage distribution characteristics of the surrounding rock deformation of the repeated mining roadway.

4.1. Distribution Characteristics of Stress Stages in Repeated Mining Roadway. The roadway with double-lane layout will be affected by repeated mining. The process of mining 0–1000 m in the coal-mining face 22204 and 0–500 m in the coal-mining face 22205 is simulated, and the maximum and minimum principal stress and difference of principal stress at monitoring face position are extracted every 100 m advancing, as shown in Figure 7.

As shown in Figure 7(a), in the process of primary mining, when the coal-mining face advances from 0 m to 300 m away from the open-off cut, the maximum and minimum principal stress change curve presents a single peak distribution, and the peak value is located in the middle of the goaf, and with the expansion of the goaf, the peak value gradually increases. When the coal-mining face advances to 400 m, the peak value of the principal stress in the lane retaining reaches the maximum, and the maximum principal stress increases from 11.7 MPa to 16.2 MPa; the peak value of minimum principal stress increases from 9.3 MPa to 11.5 MPa, and the principal stress difference is the smallest, which is about 2.3 MPa. With the continuous mining of the coal-mining face, the stress recovery range in the central part of the goaf is gradually enlarged, and the relative stress range of the retained roadway relative to the central part of the goaf is gradually expanded, but the stress value does not rise. When the coal-mining face is 0–200 m away from the stop line, the maximum principal stress decreases from the peak value to the level before mining.

As shown in Figure 7(b), in the process of second mining, when the coal-mining face advances from 0 m to 200 m away from the open-off cut, the maximum principal stress value is 0–10 m in front of each coal-mining face, the peak value of principal stress gradually increases, the maximum principal stress increases from 22 MPa to 32 MPa, and the minimum principal stress presents a single peak distribution form of first rising and then decreasing. The leading peak value increases from 13.5 MPa to 15 MPa, and the principal stress difference is different. The peak value increases from 14 MPa to 20 MPa, and the leading influence range is about 100 m; when the coal-mining face advances from 300 m to 800 m, the peak value and leading influence range almost do not change, but with the advance of the coal-mining face, the maximum principal stress value curve of second mining tends to be stable, which is consistent with the primary mining stress. Compared with the stress curve of primary mining, the stress value in the stable stage is higher than that in the stable stage of primary mining; with the continuous advance of the coal-mining face, when the distance from the stoppage line is 200 m to the stop line, the principal stress gradually decreases until it returns to the original rock stress state.

To sum up, with the advance of coal-mining face, the stress distribution of gob retaining roadway has obvious stages, which are stage I, the stability stage of mining influence, coal-mining face advancing 0–300 m, the stress increases in single peak until reaching the peak value; stage II, the expansion stage of primary mining, when the coal-mining face is 0–200 m away from the final mining line, the stress decreases from the peak to the level before mining;

TABLE 3: Material mechanics parameters for caved rock.

Bulk modulus (GPa)	Shear modulus of elasticity (GPa)	Density kg/m^{-3}	The angle of internal friction ($^\circ$)	Dilatancy angle ($^\circ$)
5.53	4.62	1800	20	7

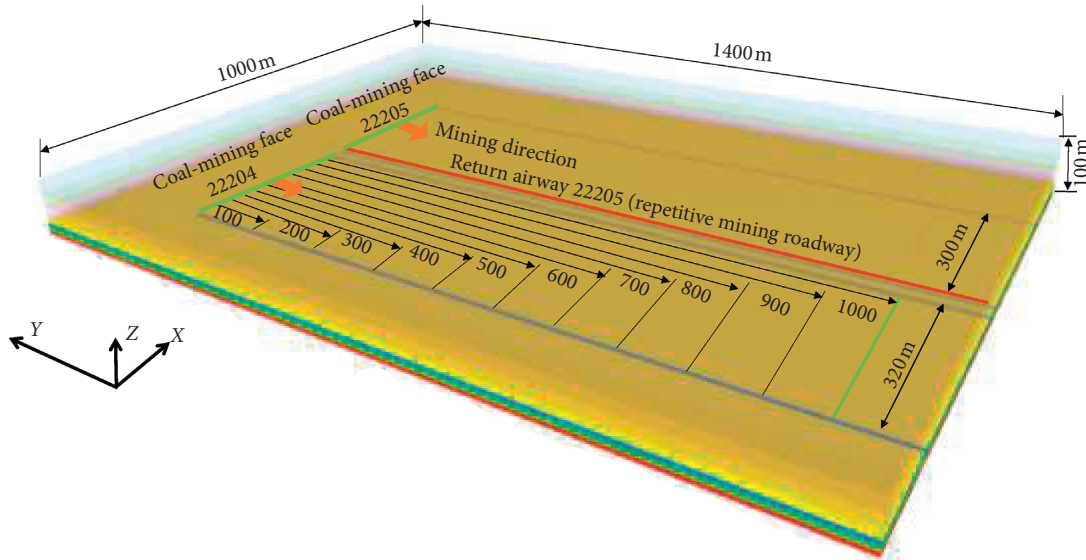


FIGURE 5: Numerical calculation model.

TABLE 4: Rock mechanics parameters of the computation model.

Lithology	Bulk modulus (GPa)	Shear modulus of elasticity (GPa)	Density kg/m^{-3}	Cohesion (MPa)	The angle of internal friction ($^\circ$)	Tensile strength (MPa)
Fine-grained sandstone	5.4	2.5	2500	15	39	2.67
Medium-grained sandstone	4.4	2.5	2500	4.6	32	1.7
Sandy mudstone	2.5	1.5	2440	3	27	0.95
2 ⁻² coal	2.2	1.5	1500	2.5	26	0.65
Sandy mudstone	2.5	2	2440	3.2	28	0.9
Siltstone	4.5	2.3	2500	1.2	33	2
Fine-grained sandstone	6.6	3.2	2500	1.4	35	2.67

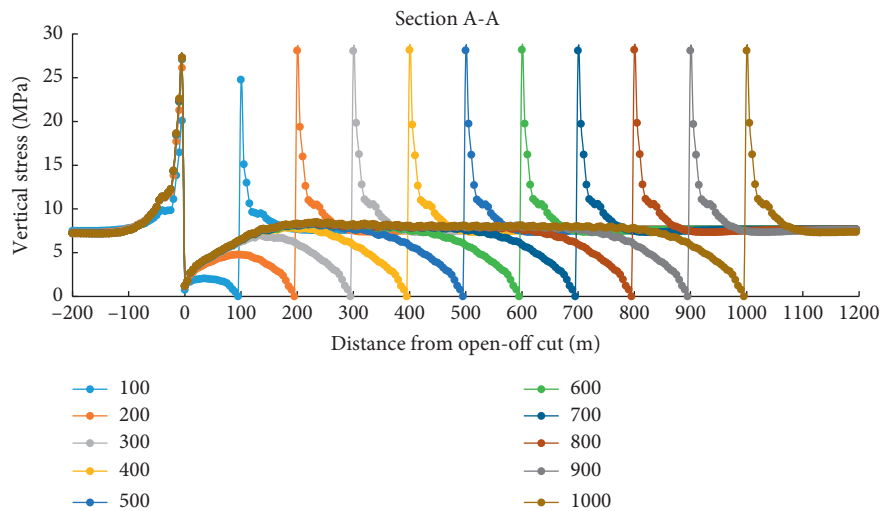


FIGURE 6: Vertical stress distribution along the goaf in the middle of the coal-mining face.

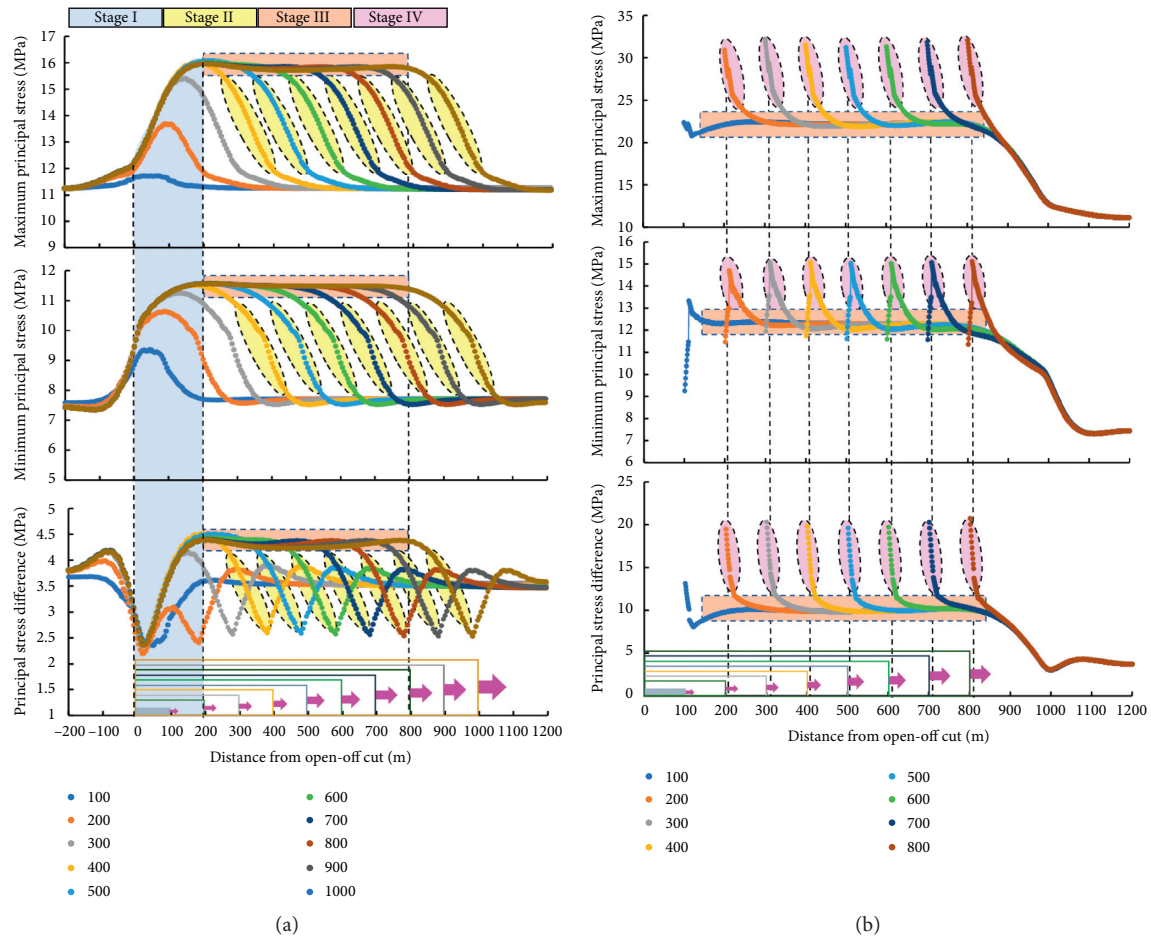


FIGURE 7: Distribution characteristics of repeated mining stress stages. (a) The primary mining. (b) The second mining.

stage III, the stable stage after primary mining, this stage is composed of two parts: after the primary mining face advances to 400 m, with the continuous advance of the coal-mining face, the stress range of the left roadway relative to the middle of the goaf gradually expands, but the stress value remains unchanged. After the second mining, with the coal-mining face advancing to 200 m before the stop line, the stress value remains unchanged, and the advanced stress range moves forward. This stage has the same characteristics with stage III in primary mining, only due to the influence of the goaf after the primary mining, the second mining stress value is higher than the primary mining stress value; stage IV, the expansion stage of the second mining, the second mining is 0–10 m away from each coal-mining face, and the stress gradually decreases from the maximum value to about 100 m in front of the coal-mining face, and the stress changes tend to be gentle.

4.2. Distribution Characteristics of Stress Stages in Fixed Monitoring Position of Roadway. In the process of repeated mining, the stress distribution of roadway retaining has obvious stages. In order to further comprehensively analyze the stress distribution regularity of the roadway with the advancing of the coal-mining face, three representative

characteristic positions 100 m, 500 m, and 900 m away from the open cut are selected as the monitoring points in the air return roadway of coal-mining face 22205 to monitor the stress change in the whole process of advancing the coal-mining face at the fixed position. The location of monitoring points is shown in Figure 8, and Figure 9 shows the stress phase diagram of each monitoring point along with the propulsion.

Compared with the stress distribution of the three monitoring points in Figure 9, it can be seen that during the primary mining process, the roadway is affected by the excavation, and the roadway is in stage I. The maximum and minimum principal stress and the principal stress difference of each monitoring point are approximately constant, while the monitoring point I is too close to the open-off cut to clearly separate stage I. During the process from 100 m before the monitoring point to 300 m behind the monitoring point, the maximum and minimum principal stress of the roadway gradually increases, and the principal stress difference will be slightly decreased in each stage. This is because the increase of the minimum principal stress is greater than the maximum principal stress, but the overall trend is also increasing. This stage is in stage II, but the monitoring point III is close to the stop line, and this stage is insufficient. During the process from 300 m to 100 m before the

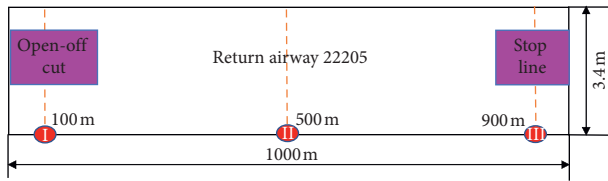


FIGURE 8: Layout of tunnel monitoring points.

monitoring point, the stress tends to be stable. Similarly, due to the influence of goaf after primary mining, the principal stress of roadway increases. Therefore, there is stress superposition between primary mining and second mining. The principal stress remains constant in the second mining stage, and the stress changes in this stage, so this stage belongs to stage III. In the process of advancing from 100 m before the monitoring point to the monitoring point, the maximum principal stress at the measuring point rises sharply and the minimum principal stress drops sharply. Therefore, the principal stress difference increases greatly and the risk of roadway damage increases. This stage is in stage IV.

To sum up, through the analysis of the stress data obtained from the three monitoring points, the stress stage distribution characteristics of each monitoring point are consistent with the stress stage in the process of repeated mining. Among them, the 500 m monitoring point can fully reflect the dynamic stress change during the whole process of coal-mining face advancing. Therefore, the specific characteristics of 500 m position stage change are discussed in detail below.

4.3. Distribution Characteristics of Plastic Zone Stage in Repeated Mining Roadway. The expansion of the plastic zone directly reflects the damage degree and scope of the surrounding rock of the roadway, so the plastic zone in the repeated mining process is extracted to explore its evolution regularity. The layout of monitoring points is the same as above. The position is selected 500 m away from the open-off cut to obtain the shape map of its plastic area change with each 100 m of advance in the process of coal-mining face advancement for detailed analysis. Figure 10 shows the stage change map of the plastic area of the reserved roadway at the position 500 m away from the open cut.

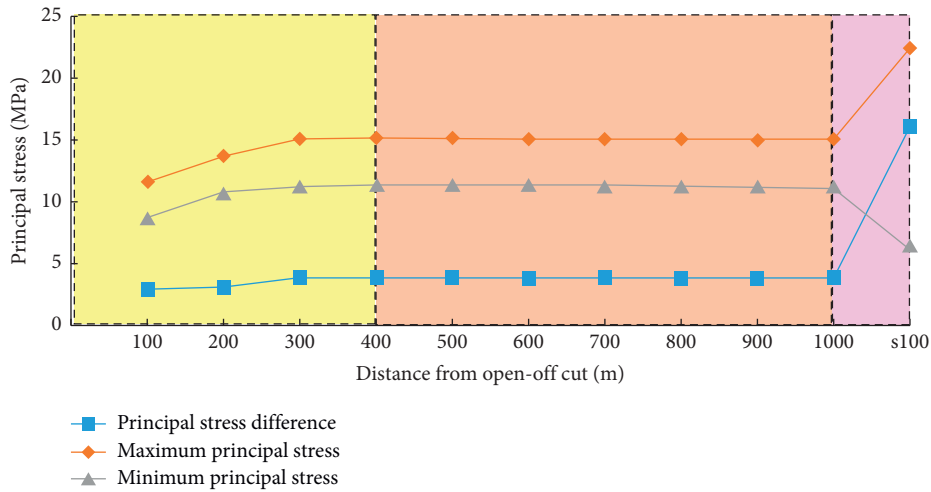
As shown in the figure, in the process of the coal-mining face advances from 100 m to 400 m away from the open-off cut in the primary mining, the change of roadway plastic zone belongs to stage I. During the coal-mining face advancing 100–200 m, the scope and shape of plastic zone did not change. In the process of coal-mining face advancing from 200 m to 300 m, the plastic zone of roadway showed that the failure range of roof and floor was almost unchanged, and the scope of two sides did not change at this time. In the process of coal-mining face advancing from 400 m to 800 m, the plastic zone of monitoring point is in stage II. In the process of coal-mining face advancing from 500 m to 600 m, the range of plastic zone of monitoring point is gradually expanded, the range of plastic zone of roof

and floor is increasing, the depth of plastic zone of roof is expanded from 2 m to 3 m, the range of plastic zone of floor is enlarged, and the range of both sides is expanded. The expanded range of coal pillar side is larger than that of coal wall, the depth is expanded from 1 m to 3 m, and the depth of coal wall is expanded from 1 m to 2 m. During the coal-mining face advancing from 600 m to 800 m, the shape of plastic zone did not change, and its scope was further expanded. In the process of coal-mining face advancing 800–1000 m away from open-off cut and second mining face 100–400 m away from open-off cut, the shape of plastic zone at this stage of monitoring point is basically consistent, and it is in stage III. During the period from 400 m to 500 m, the plastic zone of roadway is in stage IV. In this stage, the damage range and the shape of plastic zone of roadway change rapidly. The plastic zone of roadway roof is connected with coal wall, the damage range of floor increases to 3.5 m, the range of plastic zone of coal pillar is expanded rapidly, and the depth has reached 4.5 m. To sum up, with the advance of the coal-mining face, the change of the plastic zone of the monitoring position adapts to the stress distribution stage.

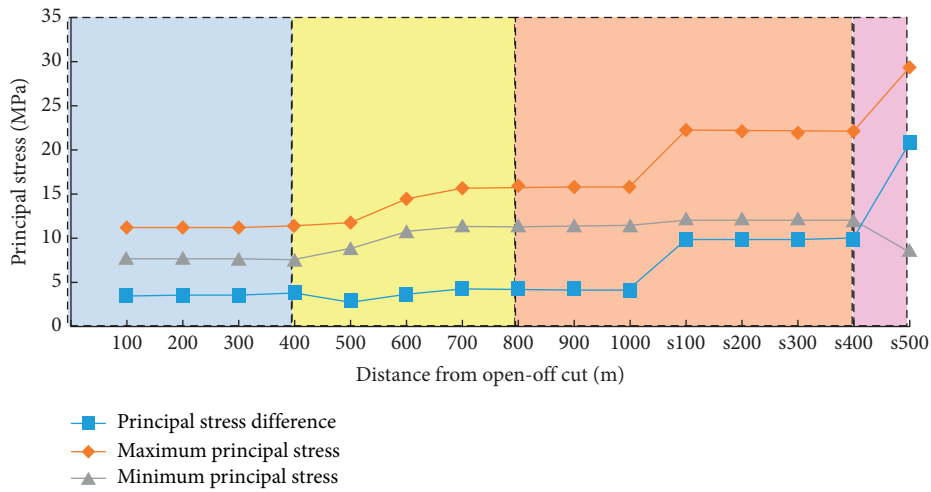
4.4. Distribution Characteristics of Displacement Stage of Surrounding Rock Surface in Repeated Mining Roadway. The surface displacement of surrounding rock can analyze the deformation regularity of surrounding rock and obtain the information of its stability, displacement monitoring is carried out for return airway 22205, and the location of roadway monitoring point is the same as above. According to the above analysis of the plastic zone of the roadway, the roadway damage mainly occurs in the roof. Therefore, a point is selected at the center of the roof and a point is selected on both sides of the roof to reduce the random error. The center point is taken at the bottom and the two sides of the roadway, respectively. Figure 11 shows the specific layout of the measuring points.

According to the data obtained by comparison, the position of 500 m monitoring point is representative. Therefore, the position displacement data of 500 m monitoring point are selected for detailed analysis below. Figure 12 shows the displacement diagram of roof, two sides, and floor of the roadway 500 m away from the opening monitoring point.

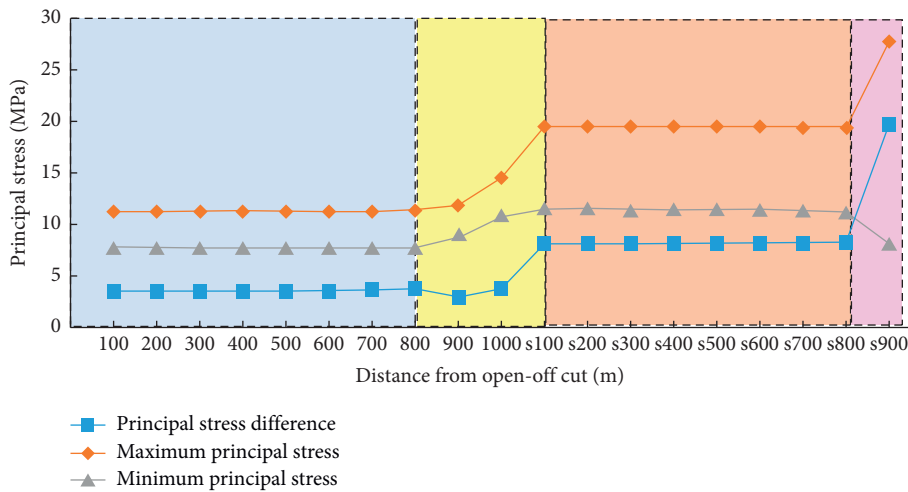
In the process of coal-mining face advancing 100–400 m, the deformation of surrounding rock of return air roadway in 22205 coal-mining face remained almost unchanged. In this stage, the roadway was mainly affected by mining, and the roadway was in stage I. In the process of coal-mining face advancing 400–800 m, the deformation of each measuring point kept increasing, and there was little difference in the displacement among the three measuring points of roof, and the retained roadway was in stage II. In the process of coal-mining face advancing 800–1000 m and second mining coal-mining face 100–400 m, the deformation of surrounding rock of roadway has a stable platform period, and the deformation of roadway surrounding rock is no longer increased.



(a)



(b)



(c)

FIGURE 9: Stress stage diagram of each monitoring point. (a) The monitoring point. (b) The monitoring point. (c) The monitoring point.

At this time, the roadway is in stage III. In the process of advancing 400–500 m of second mining face, the deformation of surrounding rock of roadway increases rapidly,

and the roadway is in stage IV. To sum up, the deformation stages of six measuring points in the process of repeated mining are consistent with the changes of stress

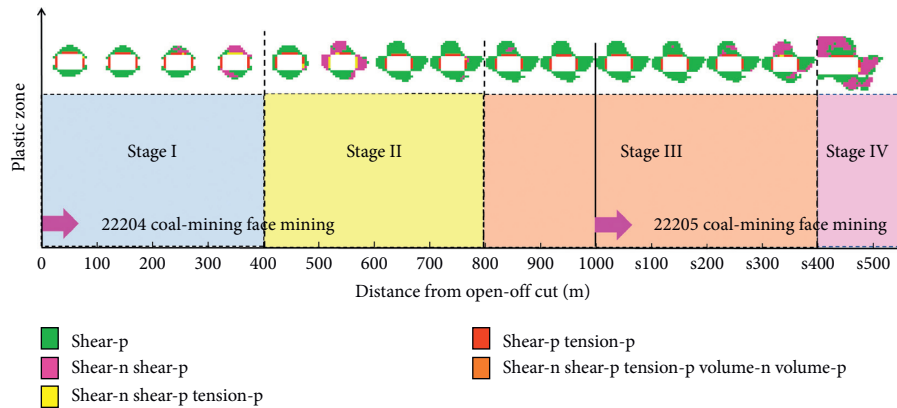


FIGURE 10: Stage change diagram of plastic zone in reserved roadway 500 m from the open-off cut.

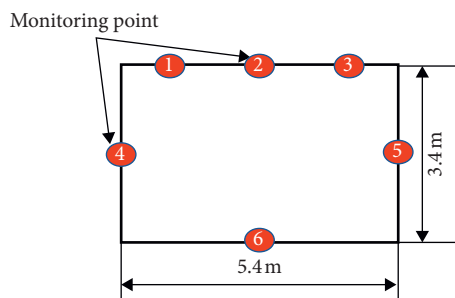


FIGURE 11: Schematic diagram of measuring points on roadway surface.

and plastic zone. In the four stages, the deformation trend of surrounding rock is the same, but the deformation of each position is different. The deformation of roof is the largest, followed by two sides. In the two sides, the deformation of the coal pillar side is greater than that of coal wall, and the deformation of floor is the smallest.

5. Deformation Mechanism and Stability Control of Surrounding Rock in Repeated Mining Roadway

5.1. Deformation Mechanism of Surrounding Rock in Repeated Mining Roadway. The essence of deformation and failure of surrounding rock is the result of formation and expansion of plastic zone. With the advance of the coal-mining face, the plastic zone of the surrounding rock of the roadway is changed by the magnitude and direction of the principal stress, which makes its extension range and shape unfixed. Figure 13 shows the shape of plastic zone under the change of principal stress deflection angle of surrounding rock of circular and rectangular tunnels under numerical simulation.

As shown in the figure, the shape and range of the butterfly plastic zone of circular or rectangular tunnels have not changed significantly in the process of deflection of the principal stress direction from 0° to 180° . However, the butterfly part of the plastic zone deflects with the deflection of the principal stress direction. When the principal stress

deflection angle turns to 180° , the shape of the plastic zone is the same as that of the nondeflection. It is precise because of the change of the direction of the principal stress that the direction of the plastic zone changes, which leads to the asymmetry of the surrounding rock failure in the actual engineering. As shown in Figure 14, the shape of plastic zone changes when the coal-mining face is mined to 400 m, 600 m, and 800 m under the condition of one mining under the background of the project.

As shown in the figure, when the primary mining face is pushed to 200 m–600 m, the maximum principal stress increases from 11.2 MPa to 14.5 MPa, the minimum principal stress increases from 7.7 MPa to 10.8 MPa, the principal stress difference increases from 3.5 MPa to 3.7 MPa, and the extension range of plastic zone gradually expands. When the primary mining face is pushed to 600 m–800 m, the maximum principal stress increases from 14.5 MPa to 15.8 MPa, the minimum principal stress increases from 10.8 MPa to 11.5 MPa, the principal stress difference increases from 3.7 MPa to 4.3 MPa, the extension range of plastic zone continues to deepen, roof and coal wall expand each other, and floor and coal pillar expand each other, which makes the tunnel asymmetric deformation more obvious. With the advance of the coal-mining face, the angle between the maximum principal stress and the vertical direction deflects from 90° to 43° anticlockwise, the shape of the plastic zone changes from symmetry to asymmetry, and the scope of the plastic zone of the top and bottom plates and the two sides also expands gradually. When the included angle deflects from 43° to 39° , because the deflection angle is not large, the orientation of the plastic zone does not change significantly. In conclusion, the deformation mechanism of the surrounding rock of the repeated mining roadway is that the increase of the principal stress difference causes the expansion of the plastic area, and the deflection of the principal stress angle causes the deflection of the expansion direction of the plastic area. Under the joint action of the magnitude of the principal stress difference and the deflection of the stress direction, the plastic area of the roadway produces a non-symmetric distribution state, leading to the asymmetric deformation and destruction of the surrounding rock of the roadway, which is also the stability of the roadway. Control makes it more difficult.

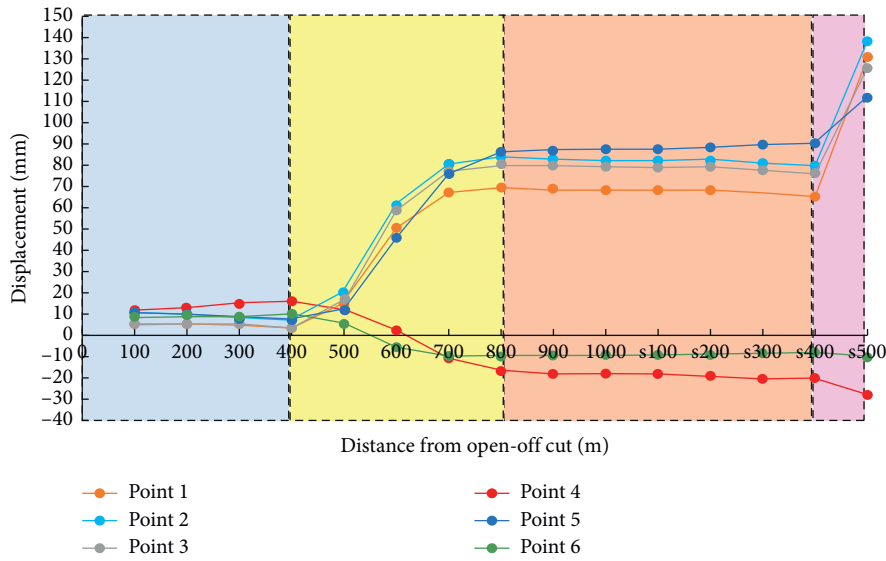


FIGURE 12: Displacement of monitoring point 500 m from the open-off cut.

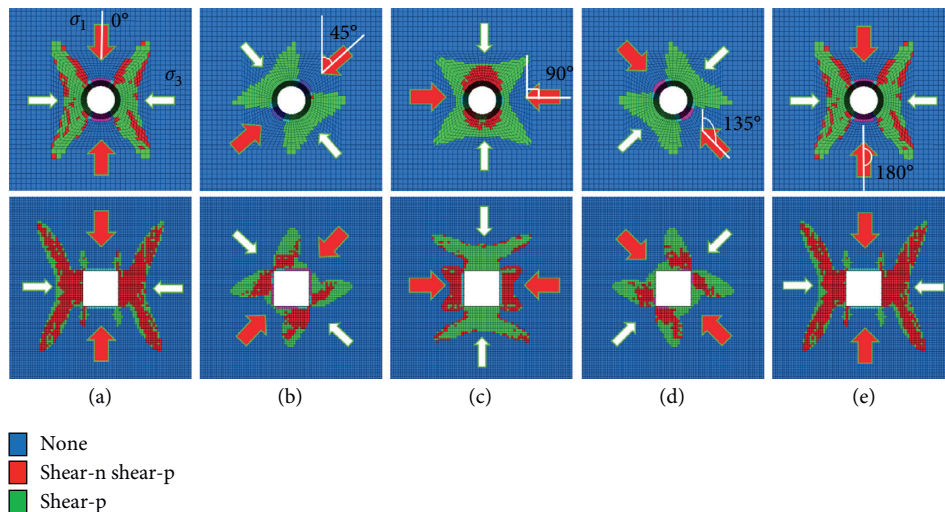


FIGURE 13: The shape of plastic zone under the change of principal stress deflection angle of surrounding rock of circular and rectangular tunnels under numerical simulation. (a) $\alpha = 0^\circ$. (b) $\alpha = 45^\circ$. (c) $\alpha = 90^\circ$. (d) $\alpha = 135^\circ$. (e) $\alpha = 180^\circ$.

5.2. Stability Control Method of Surrounding Rock in Repeated Mining Roadway. In order to better control the stability of the deformation and failure of the repeated mining roadway, according to the stage of the position of the repeated mining roadway along with the advance of the coal-mining face, the corresponding roadway control measures can be put forward in different stages.

Stage I is the stage of mining affecting stability. In the tunneling stage, the surrounding rock of the roadway is simply affected by the ground stress, and the damage scope of the plastic zone is small in a symmetrical form. The deformation of the roof and floor is large, the deformation of the coal wall and pillar is small, and the middle depth of the roof and floor is the largest. Therefore, on-site support should be based on bolt support combined with longitude and latitude network to control the shallow stability of

surrounding rock [36, 37]; at the same time, anchor cables should be arranged in the middle of the roof to prevent local roof falling accidents.

Stage II is the stage of primary mining expansion. During the primary mining period, the plastic zone of surrounding rock of roadway is mainly damaged in an asymmetric way, and the damage range and depth increase greatly, which exceeds the length of bolt support. Before mining, the anchor cables on both sides of the roof shall be supplemented, and the side anchor cables shall be added in the middle and upper part of the two sides, so as to adapt to the safety and stability of the surrounding rock during the influence of the primary mining.

Stage III is the stable stage after the primary mining. After the primary mining disturbance, the depth of the plastic zone reaches the maximum, and the scope and shape

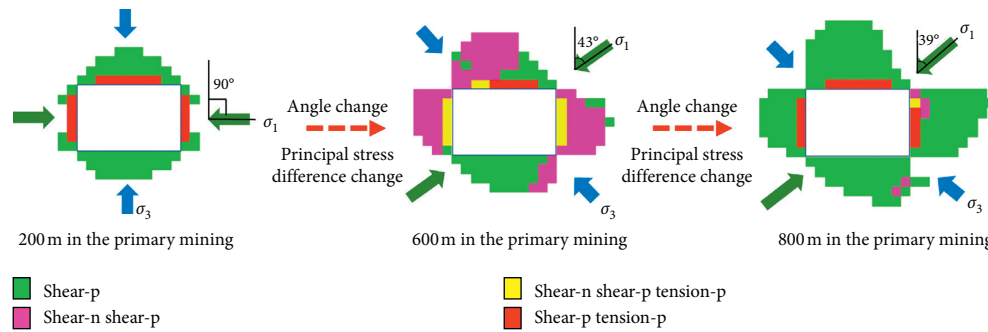


FIGURE 14: The shape of plastic zone changes when the coal-mining face is mined to 400 m, 600 m, and 800 m under the condition of the primary mining under the background of the project.

will not change for a long time. It has a long existence time and a large range of roadways. Before the second mining, there will be a phenomenon of stress superposition. Therefore, before the second mining disturbance, the surrounding rock of the roadways in this area is seriously deformed and damaged and the support body is damaged to a large extent, so roof reinforcement and support should be carried out to prevent the second mining disturbance roof fall accident occurs due to disturbance.

Stage IV is the stage of second mining expansion. During the second mining disturbance, the expansion of the plastic zone of the roadway near the coal-mining face started, and the more close to the coal-mining face, the more dramatic changes in the failure deformation set. The failure mode of the plastic zone of the surrounding rock of the roadway continued to expand to the asymmetric form, with a small increase in the depth of failure and a large increase in the scope of failure. The failure and deformation of the surrounding rock at the top corner of the coal wall and the bottom corner of the coal pillar were serious. Therefore, the support parameters after reinforcement should meet the change of the shape of the plastic zone, and the hydraulic support should be arranged in the area near the coal-mining face to prevent the surrounding rock of the roadway from destroying and causing the instability of the surrounding rock of the roadway.

According to the above research and field observation, the design of supporting parameters of return airway 22205 can meet the requirements of influencing stability stage of driving and influencing stability area of driving, but it cannot guarantee the depth control of two-side failure of surrounding rock in one mining roadway. Therefore, after driving and before the primary mining, the row distance between the middle and upper part of two sides is 850×2000 mm, $\Phi 22 \times 6500$ mm anchor cable is used, and the primary row is 1000 mm away from the roof.

5.3. Detection of Rock Failure Pattern in the Stable Stage after the Primary Mining. After the influence of a mining operation on the roadway, the field observation found that in the area about 260–1200 m behind the stopping line of the coal-mining face 22204, the surrounding rock was most damaged and deformed, and the failure forms of the roof anchor cable were broken and dropped at the lock end; anchor cable and lock fell

off, and anchor cable and lock were pulled into the coal body as a whole, without roof falling, which indicated that the design parameters of roadway support could be full. In order to prevent roof falling accident in second mining, reinforcement and support measures should be taken in stage III.

Based on the phased existence of the surrounding rock failure of the roadway, the deepest failure of the roadway is located about 500 m behind the coal-mining face, and then, the drilling peep is used to detect the depth and shape of the fracture in the hidden danger area. Due to the limitations of the surrounding rock conditions and drilling working conditions of the two sides, the peep results are not clear, so only the roof is detected, which provides the basis for the design of reinforcement support parameters. The layout scheme of borehole peep and the results of peep are shown in Figure 15.

According to the peeping results, the range A is within 0–1 m from the roof, the surrounding rock in each peephole is seriously broken, the wall of the peephole is rough, the range B is within 1–4 m, there are many cracks, the range C is within 4–8 m, the peephole wall is relatively complete, there is no crack development, and there are some irregular coal lines; from the range B, it can be seen that the local fracture development of the left borehole is concentrated on the right side, the middle borehole is multidirectional fracture, and the right borehole is The pores and fissures are fully developed, in circular and compound form. Combined with the characteristic diagram of plastic zone, it can be seen that the surface of roadway is mainly shear tensile failure, and the interior of surrounding rock is mainly shear failure. The roof is affected by the movement of overlying rock near the coal-mining face on the right side, the magnitude and direction of the principal stress change, and the surrounding rock of roof develops obviously to the left side of the coal wall. The fracture of the roof is asymmetric, and the failure depth of the side near the coal wall is greater than that of the side near the coal pillar.

5.4. Parameters and Control Effect of Reinforcement Support. According to the field observation of the deformation of surrounding rock and the failure form of the support body, combined with the previous results, it can be seen that the plastic failure depth of surrounding rock affected by the primary mining in the reserved roadway can reach about

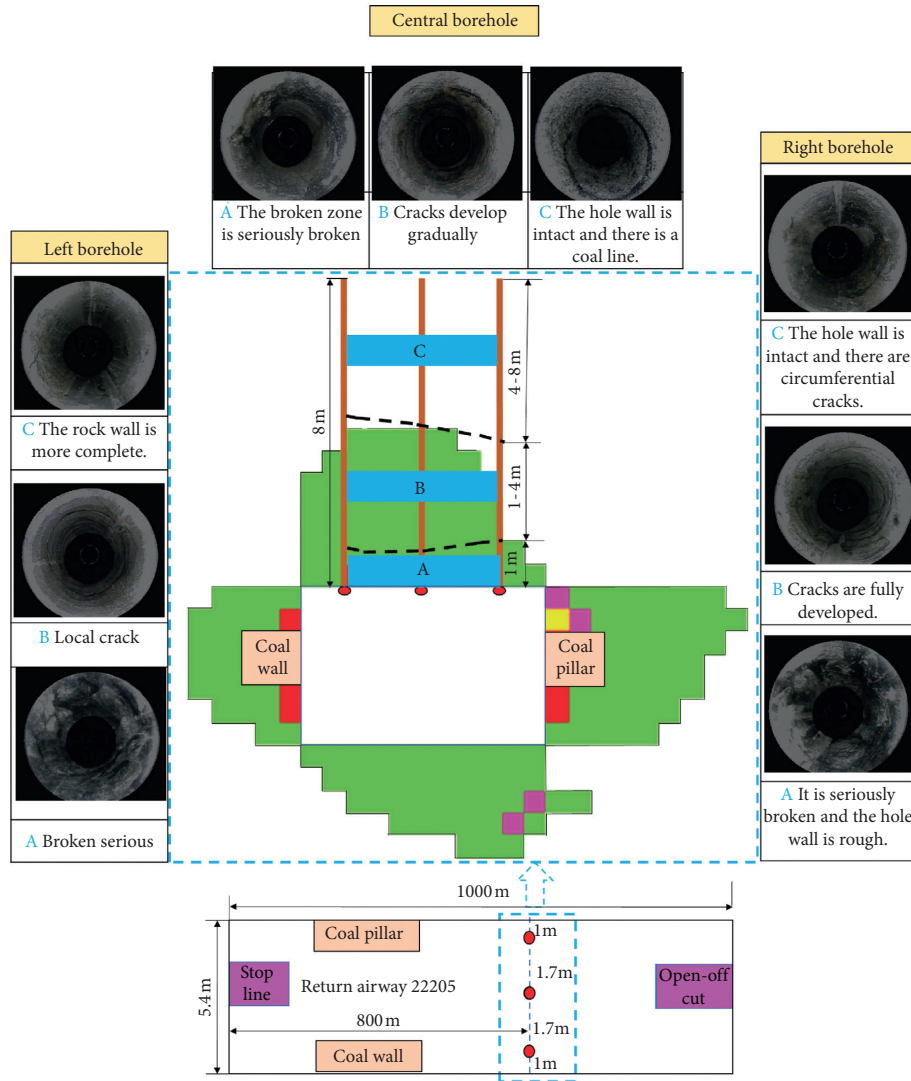


FIGURE 15: Layout scheme of borehole peep and the results of peep.

5 m, and the failure depth of surrounding rock does not exceed the anchoring range of anchor cable. Although the failure range of surrounding rock in the second mining is larger, the depth change is not large. Therefore, the reinforcement of roof with an 8 m anchor cable can meet the support requirements.

The reinforcement scheme for the area with potential roof fall hazard is as follows: $\Phi 22 \times 8000$ mm anchor cable is used, and on the basis of three original anchor cables in a row, two anchor cables are added to make up five anchor cables in a row, and three anchor cables in a row are added in the middle of each two rows, with the spacing of 2100×2000 mm, finally forming the “3, 5, 3, 5” shape, with the spacing of 1 m, with the construction of $200 \times 140 \times 8$ mm tray pressing steel belt. The roof reinforcement support is as shown in Figure 16.

After roof reinforcement, three groups of 4 m and 8 m displacement observation stations are set up in the area of roof falling hidden danger. The distance between stations is 100 m. The displacement monitoring is carried out continuously for 18

days in the middle of roof. Figure 17 shows the layout and results of the roof separation monitoring station.

As shown in the figure, through the analysis of the displacement curve of multibase points of the roof after the reinforcement of three positions, it can be seen that in the first eight days, each monitoring point has a small amount of subsidence of 3 mm–8 mm, and after eight days, it tends to be stable without any change. In the whole observation period, the subsidence of the shallow roof is higher than that of the deep. Compared with the peep of the roof, it can be seen that the surrounding rock is relatively broken within 5 m, and the roof reinforcement with anchor cable can effectively control the collapse of the broken surrounding rock, and there is no roof falling accident during the second mining.

6. Conclusion

- (1) Based on the analysis of the stress changes of the roadway affected by the repeated mining along with the advance of the coal-mining face, the mining

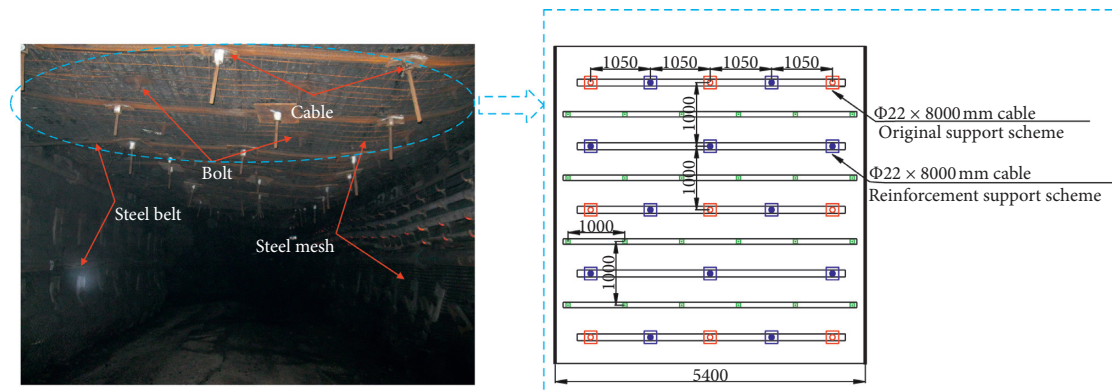


FIGURE 16: Reinforcement support parameter of roadway roof.

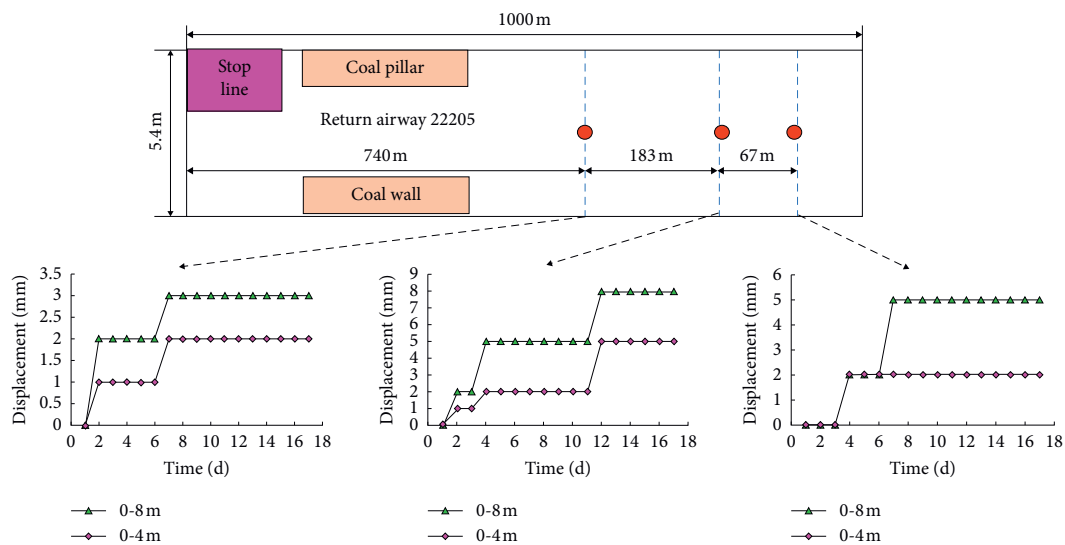


FIGURE 17: Multipoint displacement curve after reinforcement support.

- process can be roughly divided into four stages: the stability stage of mining influence, the expansion stage of primary mining, the stable stage after primary mining, and the expansion stage of second mining. At the same time, the shape changes of the plastic zone and the displacement monitoring results of the monitoring points during the mining process are analyzed, and the results are obtained; the stage of stress change is suitable.
- (2) According to the study on the plastic zone and displacement monitoring of surrounding rock, the surrounding rock of the roadway is broken into symmetrical distribution in the stage of mining affecting stability, and the top and floor are broken more than two sides. The plastic zone is broken more deeply in the stage of primary mining expansion, which is asymmetrical distribution. The plastic zone depth reaches the maximum in the stable stage after the primary mining, and the roof deformation is the largest, and the coal pillar deformation is larger than

the coal wall. The stage of second mining expansion is closer to the coal-mining face, and its plastic zone damage deformation is more intense.

- (3) Through numerical simulation, it is concluded that the deformation mechanism of the surrounding rock of the repeated mining roadway is that the increase of the principal stress difference makes the plastic area expand, and the deflection of the principal stress angle makes the plastic area expand. Under the combined action of the stress magnitude of the principal stress difference and the deflection of the stress direction, the plastic area of the roadway produces an asymmetrical distribution state, which leads to the asymmetric deformation and destruction of the surrounding rock of the roadway.
- (4) Based on the analysis of the stage characteristics of the driving process of the repeated mining roadway, it is proposed that the reinforcement and support measures should be taken in stage III, and the specific reinforcement scheme should be determined

according to the expansion form of the plastic area and the field measurement; the roof reinforcement and support should be carried out to ensure the production safety.

Data Availability

The data used to support the findings of this study are available from the corresponding author upon request.

Conflicts of Interest

The authors declare that there are no conflicts of interest regarding the publication of this paper.

Acknowledgments

This research was supported by the National Natural Science Foundation of China (grant nos. 51964036 and 51764044), Natural Science Foundation of Inner Mongolia (grant nos. 2019LH05004 and 2019MS05055), Innovation Fund Project of Inner Mongolia University of Science and Technology (grant no. 2019QDL-B31), and Foundation of Inner Mongolia Department of Science and Technology (grant no. 20180823).

References

- [1] X. Wang, C. Liu, S. Chen, L. Chen, K. Li, and N. Liu, "Impact of coal sector's de-capacity policy on coal price," *Applied Energy*, vol. 265, Article ID 114802, 2020.
- [2] C. Wang, B. Shen, J. Chen et al., "Compression characteristics of filling gangue and simulation of mining with gangue backfilling: an experimental investigation," *Geomechanics and Engineering*, vol. 20, no. 6, pp. 485–495, 2020.
- [3] J. Chen, J. Zhao, S. Zhang, Y. Zhang, F. Yang, and M. Li, "An experimental and analytical research on the evolution of mining cracks in deep floor rock mass," *Pure and Applied Geophysics*, vol. 2020, no. 1, pp. 1–16, 2020.
- [4] D. Liu, Z. Gu, R. Liang et al., "Impacts of pore-throat system on fractal characterization of tight sandstones," *Geofluids*, vol. 2020, Article ID 4941501, 17 pages, 2020.
- [5] H. Pan, D. Yin, N. Jiang, and Z. Xia, "Crack initiation behaviors of granite specimens containing crossing-double-flaws with different lengths under uniaxial loading," *Advances in Civil Engineering*, vol. 2020, Article ID 8871335, 13 pages, 2020.
- [6] J. Wang, Y. Zhang, Z. Qin, S. Song, and P. Lin, "Analysis method of water inrush for tunnels with damaged water-resisting rock mass based on finite element method-smooth particle hydrodynamics coupling," *Computers and Geotechnics*, vol. 126, Article ID 103725, 2020.
- [7] D. Ren, D. Zhou, D. Liu, F. Dong, S. Ma, and H. Huang, "Formation mechanism of the Upper Triassic Yanchang Formation tight sandstone reservoir in Ordos Basin-Take Chang 6 reservoir in Jiyuan oil field as an example," *Journal of Petroleum Science and Engineering*, vol. 178, pp. 497–505, 2019.
- [8] G. Feng, X. C. Wang, M. Wang, and Y. Kang, "Experimental investigation of thermal cycling effect on fracture characteristics of granite in a geothermal-energy reservoir," *Engineering Fracture Mechanics*, vol. 235, Article ID 107180, 16 pages, 2020.
- [9] G. Feng, Y. Kang, X. Wang, Y. Hu, and X. Li, "Investigation on the failure characteristics and fracture classification of shale under brazilian test conditions," *Rock Mechanics and Rock Engineering*, vol. 53, no. 7, pp. 3325–3340, 2020.
- [10] J. Xu, A. Haque, W. Gong et al., "Experimental study on the bearing mechanisms of rock-socketed piles in soft rock based on micro X-ray CT analysis," *Rock Mechanics and Rock Engineering*, vol. 53, no. 8, pp. 3395–3416, 2020.
- [11] H. Kang, L. Yan, X. Guo et al., "Characteristics of surrounding rock deformation and reinforcement technology of retained entry in coal-mining face with multi-entry layout," *Chinese Journal of Rock Mechanics and Engineering*, vol. 31, no. 10, pp. 2022–2036, 2012.
- [12] S. Wang, D. Mao, J. Pan et al., "Measurement on the whole process of abutment pressure evolution and microseismic activities at the lateral strata of goaf," *Journal of China Coal Society*, vol. 40, no. 12, pp. 2772–2779, 2015.
- [13] X. Zhang, "Study on deformation law of surrounding rock of roadway under the influence of the two mining," *Modern Mining*, vol. 26, no. 8, pp. 113–115, 2010.
- [14] J. Liu, E. Wang, E. Zhao et al., "Distribution and variation of mining-induced stress field in deep workforce," *Journal of Mining & Safety Engineering*, vol. 31, no. 1, pp. 60–65, 2014.
- [15] X. Yu, Q. Wang, B. Zhao et al., "Study on reasonable width of pillar between roadways in large mining heigh face with double roadways layout," *Chinese Journal of Rock Mechanics and Engineering*, vol. 34, no. Sup 1, pp. 3328–3336, 2015.
- [16] S. Hou, H. Jing, and D. Yang, "Physical model for deformation-failure evolution of double gob-side entry," *Chinese Journal of Geotechnical Engineering*, vol. 33, no. 2, pp. 265–268, 2011.
- [17] X. Guo, Z. Zhao, X. Gao, X. Wu, and N. Ma, "Analytical solutions for characteristic radii of circular roadway surrounding rock plastic zone and their application," *International Journal of Mining Science and Technology*, vol. 29, no. 3, pp. 263–272, 2019.
- [18] L. Jiang, P. Zhang, L. Chen et al., "Numerical approach for goaf-side entry layout and yield pillar design in fractured ground conditions," *Rock Mechanics and Rock Engineering*, vol. 50, no. 11, pp. 3049–3071, 2017.
- [19] L. Jiang, P. Kong, P. Zhang et al., "Dynamic analysis of the rock burst potential of a longwall panel intersecting with a fault," *Rock Mechanics and Rock Engineering*, vol. 53, no. 4, pp. 1737–1754, 2020.
- [20] L. Jiang, Y. Zhao, N. Golsanami, L. Chen, and W. Yan, "A novel type of neural networks for feature engineering of geological data: case studies of coal and gas hydrate-bearing sediments," *Geoscience Frontiers*, vol. 11, no. 5, pp. 1511–1531, 2020.
- [21] G. C. Zhang, Z. J. Wen, S. J. Liang et al., "Ground response of a gob-side entry in a longwall panel extracting 17 m-thick coal seam: a case study," *Rock Mechanics and Rock Engineering*, vol. 53, no. 2, pp. 497–516, 2019.
- [22] X. Wu, H. Liu, J. Li et al., "Space-time evolutionary regularity of plastic zone and stability control in repetitive mining Roadway," *Journal of China Coal Society*.
- [23] Z. Zhang, M. Deng, J. Bai, X. Yu, Q. Wu, and L. Jiang, "Strain energy evolution and conversion under triaxial unloading confining pressure tests due to gob-side entry retained," *International Journal of Rock Mechanics and Mining Sciences*, vol. 126, Article ID 104184, 2020.
- [24] G. Zhang, L. Chen, Z. M. Wen, G. Tao, Y. Li, and H. Zuo, "Squeezing failure behavior of roof-coal masses in a gob-side

- entry driven under unstable overlying strata,” *Energy Science & Engineering*, vol. 8, no. 7, pp. 2443–2456, 2020.
- [25] E. Chen, G. Chen, X. Yang, G. Zhang, and W. Guo, “Study on the failure mechanism for coal roadway stability in jointed rock mass due to the excavation unloading effect,” *Energies*, vol. 13, no. 10, p. 2515, 2020.
- [26] B.-y. Jiang, S.-t. Gu, L.-g. Wang, G.-c. Zhang, and W.-s. Li, “Strainburst process of marble in tunnel-excavation-induced stress path considering intermediate principal stress,” *Journal of Central South University*, vol. 26, no. 4, pp. 984–999, 2019.
- [27] H. Liu, X. Wu, H. Zhen et al., “Evolution law and stability control of plastic zones of retained entry of working face with double roadways layout,” *Journal of Mining & Safety Engineering*, vol. 34, no. 4, pp. 689–697, 2017.
- [28] B. Xia, T. Gong, B. Yu, and L. Zhou, “Numerical simulation method of stope pressure in the whole process of longwall mining,” *Journal of China Coal Society*, vol. 42, no. 9, pp. 2235–2244, 2017.
- [29] M. Salamon, “Mechanism of caving in longwall coal mining. Rock mechanics contribution and challenges,” in *Proceedings of the 31st US symposium of rock mechanics*, pp. 161–168, Golden, Colorado, June 1990.
- [30] H. Yavuz, “An estimation method for cover pressure re-establishment distance and pressure distribution in the goaf of longwall coal mines,” *International Journal of Rock Mechanics and Mining Sciences*, vol. 41, no. 2, pp. 193–205, 2004.
- [31] M. Bai, F. S. Kendorski, and D. J. Van Roosendaal, “Chinese and North American high-extraction underground coal mining strata behavior and water protection experience and guidelines,” in *Proceedings of the 14th International Conference on Ground Control in Mining*, West Virginia University, Morgantown, WV, USA, August 1995.
- [32] S. S. Peng and H. S. Chiang, *Longwallminim*, Wiley, Hoboken, NY, USA, 1984.
- [33] Q. Bai, S. Tu, Y. Yuan et al., “Back analysis of mining induced responses on the basis of goaf compaction theory,” *Journal of China University of Mining & Technology*, vol. 42, no. 3, pp. 355–361, 2013.
- [34] C. Zhu, M. C. He, M. Karakus, X. B. Cui, and Z. G. Tao, “Investigating toppling failure mechanism of anti-dip layered slope due to excavation by physical modelling,” *Rock Mechanics and Rock Engineering*, vol. 2020, no. 1, pp. 1–20, 2020.
- [35] L. Jiang, Q. Wu, X. Li et al., “Numerical simulation on coupling method between mining-induced stress and goaf compression,” *Journal of China Coal Society*, vol. 42, no. 8, pp. 1951–1959, 2017.
- [36] J. Zhang, “Theoretical analysis on failure zone of surrounding rock in deep large—scale soft rock roadway,” *Journal of China University of Mining & Technology*, vol. 46, no. 2, pp. 292–298, 2017.
- [37] Y. Zhao, W. Wang, F. Zhao et al., “Strength reduction method to study safety of multilayer goafs isolation roof,” *Journal of China Coal Society*, vol. 35, no. 8, pp. 1257–1262, 2010.